# The Star Formation Newsletter

A community newsletter on Star and Planet Formation research

**No. 336** — 21 December 2020
Editor: João Alves
www.starformation.news

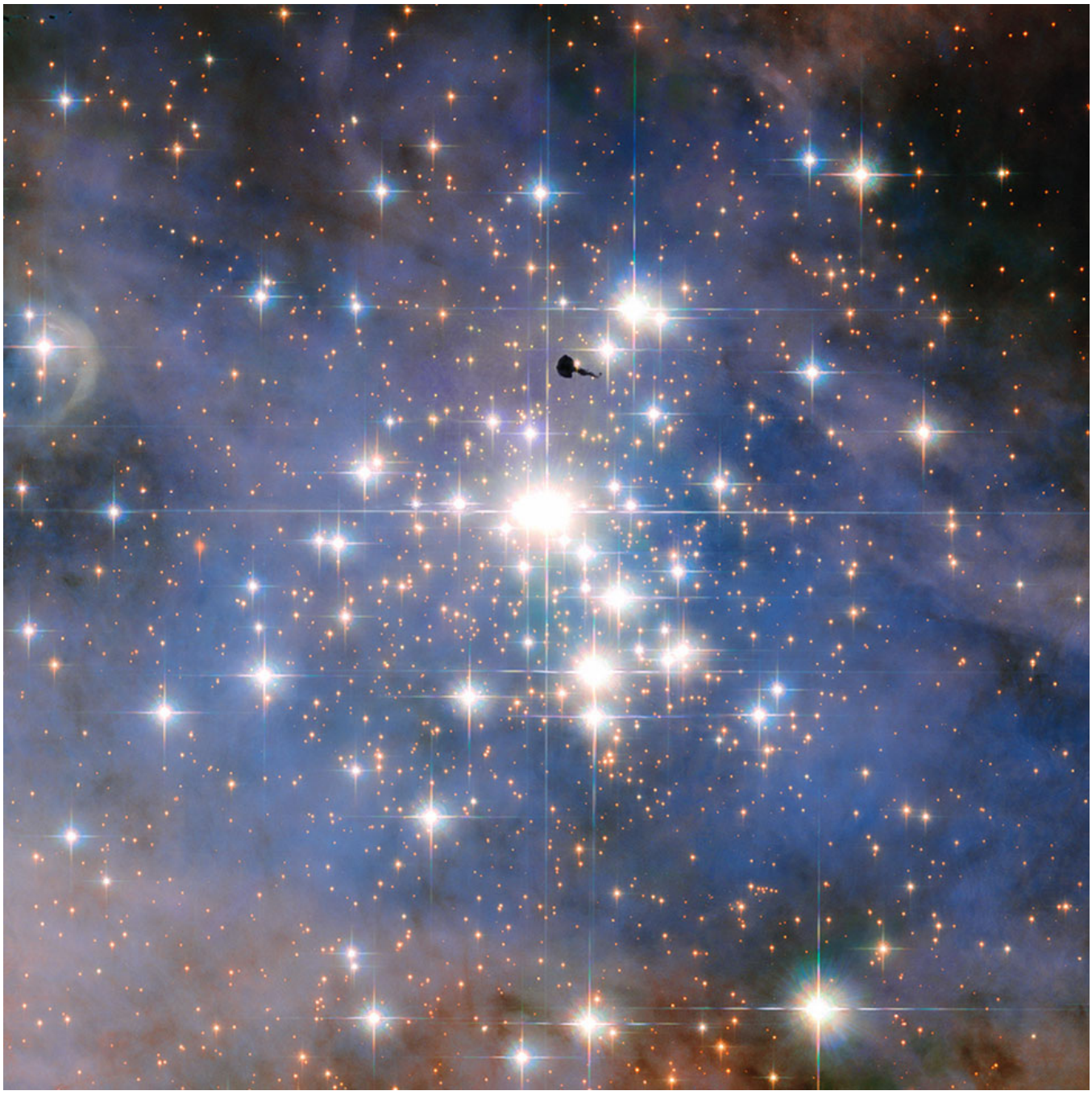

**Links to sections**



**Cover image caption**

The young cluster Trumpler 14 is one of the youngest massive star clusters in the Milky Way. With an age of about 4 Myr, a mass of the order of $10^4$ $M_\odot$, the cluster contains about 10 O-type and hundreds of B-type stars. The peculiarly shaped black spot North of the center is not an image artifact but a dense globule's silhouette. Trumpler 14 lies at a distance of about 2.8 kpc in the Carina Star-Forming Region. Credit: NASA, ESA, and J. Maíz Apellániz

**Note from the Editor**

The Star Formation Newsletter is now on the web at **www.starformation.news**. This PDF file contains the monthly Abstracts and links to the different Newsletter sections. Red text in this PDF is a url link. Submitting an abstract to the SFN is as simple as entering the arXiv ID (e.g., 2006.10139) in a web form on the SFN web site. We extract the title, authors, and the abstract's text directly from the arXiv, so make sure not to remove the LaTeX formatting when submitting to the arXiv. If you do, your abstract will not look great either at the arXiv (which uses MathJax to convert LaTeX math symbols to the web) or the SFN.

# Abstracts

1. ## Resolving the outer ring of HD 38206 using ALMA and constraining limits on planets in the system

**Mark Booth, Michael Schulz, Alexander V. Krivov, Sebastián Marino, Tim D. Pearce, Ralf Launhardt** HD 38206 is an A0V star in the Columba association, hosting a debris disc first discovered by IRAS. Further observations by Spitzer and Herschel showed that the disc has two components, likely analogous to the asteroid and Kuiper belts of the Solar System. The young age of this star makes it a prime target for direct imaging planet searches. Possible planets in the system can be constrained using the debris disc. Here we present the first ALMA observations of the system's Kuiper belt and fit them using a forward modelling MCMC approach. We detect an extended disc of dust peaking at around 180 au with a width of 140 au. The disc is close to edge on and shows tentative signs of an asymmetry best fit by an eccentricity of $0.25^{+0.10}_{-0.09}$. We use the fitted parameters to determine limits on the masses of planets interior to the cold belt. We determine that a minimum of four planets are required, each with a minimum mass of 0.64 $M_J$, in order to clear the gap between the asteroid and Kuiper belts of the system. If we make the assumption that the outermost planet is responsible for the stirring of the disc, the location of its inner edge and the eccentricity of the disc, then we can more tightly predict its eccentricity, mass and semimajor axis to be $e_{\rm p} = 0.34^{+0.20}_{-0.13}$, $m_{\rm p} = 0.7^{+0.5}_{-0.3}\,{\rm M_J}$ and $a_{\rm p} = 76^{+12}_{-13}$ au.

2. ## The Age of the Carina Young Association and Potential Membership of HD 95086

**Mark Booth, Carlos del Burgo, Valeri V. Hambaryan** Carina is a nearby young stellar association. So far, only a small number of stars have been clearly identified as members of this association. In this paper we reanalyse the membership of the association in light of Gaia DR2 data, in particular finding that HD 95086 is a potential member (probability of 71This star is noteworthy as one of the few stars that hosts both a detected debris disc and a directly imaged planet. It has previously only been considered as a potential member of the Lower Centaurus Crux (LCC) - part of the Scorpius-Centaurus association. We also reanalyse the age of the Carina association. Using a Bayesian inference code applied to infer a solution from stellar evolution models for the most probable (>99infer an age for the association of $13.3^{+1.1}_{-0.6}$ Myr, much younger than previous studies. Whilst we have revised HD 95086's association membership from LCC to Carina, the fact that we also find Carina to have a younger age, similar to that of LCC, means that the estimates of HD 95086b's mass remain unchanged. However, the younger age of Carina does mean that the companion to another Carina member, HD 44627 (or AB Pic), has a mass that is more clearly in the planet rather than brown dwarf range.

## 3. Dynamical stellar masses of pre-main sequence stars in Lupus and Taurus obtained with ALMA surveys in comparison with stellar evolutionary models

**Teresa A. M. Braun, Hsi-Wei Yen, Patrick M. Koch, Carlo F. Manara, Anna Miotello, Leonardo Testi** We analysed archival molecular line data of pre-main sequence (PMS) stars in the Lupus and Taurus star-forming regions obtained with ALMA surveys with an integration time of a few minutes per source. We stacked the data of $^{13}$CO and C$^{18}$O (J = 2-1 & 3-2) and CN (N = 3-2, J = 7/2-5/2) lines to enhance the signal-to-noise ratios, and measured the stellar masses of 45 out of 67 PMS stars from the Keplerian rotation in their circumstellar disks. The measured dynamical stellar masses were compared to the stellar masses estimated from the spectroscopic measurements with seven different stellar evolutionary models. We found that the magnetic model of Feiden (2016) provides the best estimate of the stellar masses in the mass range of 0.6 $M_\odot \leq M_\star \leq$ 1.3 $M_\odot$ with a deviation of $<0.7\sigma$ from the dynamical masses, while all the other models underestimate the stellar masses in this mass range by 20% to 40%. In the mass range of $< 0.6$ $M_\odot$, the stellar masses estimated with the magnetic model of Feiden (2016) have a larger deviation ($> 2\sigma$) from the dynamical masses, and other, non-magnetic stellar evolutionary models of Siess et al. (2000), Baraffe et al. (2015) and Feiden (2016) show better agreements with the dynamical masses with the deviations of $1.4\sigma$ to $1.6\sigma$. Our results show the mass dependence of the accuracy of these stellar evolutionary models.

## 4. $H_2$ mass-velocity relationship from 3D numerical simulations of jet-driven molecular outflows

**Adriano Cerqueira, Bertrand Lefloch, Alejandro Esquivel, Pedro Rivera-Ortiz, Claudio Codella, Cecilia Ceccarelli, Linda Podio** Previous numerical studies have shown that in protostellar outflows, the mass-velocity distribution $m(v)$ can be well described by a broken power law $\propto v^{-\gamma}$. On the other hand, recent observations of a sample of outflows show that the CO intensity-velocity distribution, closely related to $m(v)$, follows an exponential law $\propto \exp(-v/v_0)$. In the present work, we revisit the physical origin of the mass-velocity relationship $m(v)$ in jet-driven protostellar outflows. We investigate the respective contributions of the different regions of the outflow, from the swept-up ambient gas to the jet. We performed 3D numerical simulations of a protostellar jet propagating into a molecular cloud using the hydrodynamical code Yguazu-a. The code takes into account atomic and ionic species and was modified to include the $H_2$ gas. We find that by excluding the jet contribution, $m(v)$ is satisfyingly fitted with a single exponential law, with $v_0$ well in the range of observational values. The jet contribution results in additional components in the mass-velocity relationship. This empirical mass-velocity relationship is found to be valid locally in the outflow. The exponent $v_0$ is almost constant in time and for a given level of mixing between the ambient medium and the jet material. In general, $v_0$ displays only a weak spatial dependence. A simple modeling of the L1157 outflow successfully reproduces the various components of the observed CO intensity-velocity relationship. Our simulations indicate that these components trace the outflow cavity of swept-up gas and the material entrained along the jet, respectively. The CO intensity-velocity exponential law is naturally explained by the jet-driven outflow model. The entrained material plays an important role in shaping the mass-velocity profile.

## 5. The GRAVITY Young Stellar Object survey IV. The CO overtone emission in 51 Oph at sub-au scales

**GRAVITY Collaboration, M. Koutoulaki et al.** 51 Oph is a Herbig Ae/Be star that exhibits strong near-infrared CO ro-vibrational emission at 2.3 micron, most likely originating in the innermost regions of a circumstellar disc. We aim to obtain the physical and geometrical properties of the system by spatially resolving the circumstellar environment of the inner gaseous disc. We used the second-generation VLTI/GRAVITY to spatially resolve the continuum and the CO overtone emission. We obtained data over 12 baselines with the auxiliary telescopes and derive visibilities, and the differential and closure phases as a function of wavelength. We used a simple LTE ring model of the CO emission to reproduce the spectrum and CO line displacements. Our interferometric data show that the star is marginally resolved at our spatial resolution, with a radius of 10.58+-2.65 Rsun.The K-band continuum emission from the disc is inclined by 63+-1 deg, with a position angle of 116+-1 deg, and 4+-0.8 mas (0.5+-0.1 au) across. The visibilities increase within the CO line emission, indicating that the CO is emitted within the dust-sublimation radius.By modelling the CO bandhead spectrum, we derive that the CO is emitted from a hot (T=1900-2800 K) and dense (NCO=(0.9-9)$\times 10^2$1 cm$^-$2) gas. The analysis of the CO line displacement with respect to the continuum allows us to infer that the CO is emitted from a region 0.10+-0.02 au across, well within the dust-sublimation radius. The inclination and position angle of the CO line emitting region is consistent with that of the dusty disc. Our spatially resolved interferometric observations confirm the CO ro-vibrational emission within the dust-free region of the inner disc. Conventional disc models exclude the presence of CO in the dust-depleted regions of Herbig AeBe stars. Ad hoc models of the innermost disc regions, that can compute the properties of the dust-free inner disc, are therefore required.

## 6. The Explosion in Orion-KL as Seen by Mosaicking the Magnetic Field with ALMA

**Paulo C. Cortes, Valentin J. M. Le Gouellec, Charles L. H. Hull, Josep M. Girart, Fabien Louvet, Edward B. Fomalont, Seiji Kameno, George A. Moellenbrock, Hiroshi Nagai, Kouichiro Nakanishi, Eric Villard** We present the first linear-polarization mosaicked observations performed by the Atacama Large Millimeter/submillimeter Array (ALMA). We mapped the Orion-KLeinmann-Low (Orion-KL) nebula using super-sampled mosaics at 3.1 and 1.3 mm as part of the ALMA Extension and Optimization of Capabilities (EOC) program. We derive the magnetic field morphology in the plane of the sky by assuming that dust grains are aligned with respect to the ambient magnetic field. At the center of the nebula, we find a quasi-radial magnetic field pattern that is aligned with the explosive CO outflow up to a radius of approximately 12 arc-seconds ( 5000 au), beyond which the pattern smoothly transitions into a quasi-hourglass shape resembling the morphology seen in larger-scale observations by the James-Clerk-Maxwell Telescope (JCMT). We estimate an average magnetic field strength $\langle B \rangle = 9.4$ mG and a total magnetic energy of $2 \times 10^4 5$ ergs, which is three orders of magnitude less than the energy in the explosive CO outflow. We conclude that the field has been overwhelmed by the outflow and that a shock is propagating from the center of the nebula, where the shock front is seen in the magnetic field lines at a distance of $\sim 5000$ au from the explosion center.

## 7. The SEDIGISM survey: Molecular clouds in the inner Galaxy

**SEDIGISM Collaboration, A. Duarte-Cabral et al.** We use the 13CO(2-1) emission from the SEDIGISM high-resolution spectral-line survey of the inner Galaxy, to extract the molecular cloud population with a large dynamic range in spatial scales, using the SCIMES algorithm. This work compiles a cloud catalogue with a total of 10663 molecular clouds, 10300 of which we were able to assign distances and compute physical properties. We study some of the global properties of clouds using a science sample, consisting of 6664 well resolved sources and for which the distance estimates are reliable. In particular, we compare the scaling relations retrieved from SEDIGISM to those of other surveys, and we explore the properties of clouds with and without high-mass star formation. Our results suggest that there is no single global property of a cloud that determines its ability to form massive stars, although we find combined trends of increasing mass, size, surface density and velocity dispersion for the sub-sample of clouds with ongoing high-mass star formation. We then isolate the most extreme clouds in the SEDIGISM sample (i.e. clouds in the tails of the distributions) to look at their overall Galactic distribution, in search for hints of environmental effects. We find that, for most properties, the Galactic distribution of the most extreme clouds is only marginally different to that of the global cloud population. The Galactic distribution of the largest clouds, the turbulent clouds and the high-mass star-forming clouds are those that deviate most significantly from the global cloud population. We also find that the least dynamically active clouds (with low velocity dispersion or low virial parameter) are situated further afield, mostly in the least populated areas. However, we suspect that part of these trends may be affected by some observational biases, and thus require further follow up work in order to be confirmed.

## 8. Temperature Structure of the Pipe Nebula Studied by the Intensity Anomaly of the OH 18 cm

**Yuji Ebisawa, Nami Sakai, Karl M. Menten, Yoko Oya, Satoshi Yamamoto** We present observations of the four hyperfine structure components of the OH 18 cm transition (1612, 1665, 1667 and 1720 MHz) toward a filamentary dark cloud, the Pipe nebula, with the Green Bank Telescope. A statistical equilibrium analysis is applied to the spectra,and the kinetic temperature of a diffuse molecular gas surrounding dense cores is determined accurately; the derived temperature ranges from 40 K to 75 K. From this result, we assess the heating effect on the filamentarystructure of the nebula's "stem" region due to UV photons from a nearby star $\theta$-Ophiuchi and a possible filament-filament collision in the interface of the "stem" and "bowl" regions. In the stem region, the gas kinetic temperature is found to be almost independent of the apparent distance from $\theta$-Ophiuchi: the UV-heating effect by the star is not visible. On the other hand, the gas kinetic temperature is raised, as high as $\sim$75 K, at the interface of the two filamentary structures. This result provides us with an additional support to the filament-filament collision scenario in the Pipe nebula.

## 9. $^{26}$Al Enrichment in the Surface of Protostellar Disks Due to Protostellar Cosmic Rays

**Brandt A. L. Gaches, Stefanie Walch, Stella S. R. Walch, Carsten Münker** The radioactive decay of aluminum-26 ($^{26}$Al) is an important heating source in early planet formation. Since its discovery, there have been several mechanisms proposed to introduce $^{26}$Al into protoplanetary disks, primarily through contamination by external sources. We propose a local mechanism to enrich protostellar disks with $^{26}$Al through irradiation of the protostellar disk surface by cosmic rays accelerated in the protostellar accretion shock. We calculate the $^{26}$Al enrichment, [$^{26}$Al/$^{27}$Al], at the surface of the protostellar disk in the inner AU throughout the evolution of low-mass stars, from M-dwarfs to proto-Suns. Assuming constant mass accretion rates, $\dot{m}$, we find that irradiation by MeV cosmic rays can provide significant enrichment on the disk surface if the cosmic rays are not completely coupled to the gas in the accretion flow. Importantly, we find that low accretion rates, $\dot{m} < 10^{-7}$ M$_\odot$ yr$^{-1}$, are able to produce canonical amounts of $^{26}$Al, [$^{26}$Al/$^{27}$Al] $\approx 5 \times 10^{-5}$. These accretion rates are experienced at the transition from Class I- to Class II-type protostars, when it is assumed that calcium-aluminum-rich inclusions condense in the inner disk.

We conclude that irradiation of the inner disk surface by cosmic ray protons accelerated in accretion shocks at the protostellar surface may be an important mechanism to produce $^{26}$Al. Our models show protostellar cosmic rays may be a viable model to explain the enrichment of $^{26}$Al found in the Solar System.

## 10. Chamaeleon DANCe. Revisiting the stellar populations of Chamaeleon I and Chamaeleon II with Gaia-DR2 data

**P. A. B. Galli, H. Bouy, J. Olivares, N. Miret-Roig, L. M. Sarro, D. Barrado, A. Berihuete, E. Bertin, J. C. Cuillandre** Context: Chamaeleon is the southernmost low-mass star-forming complex within 200 pc from the Sun. Its stellar population has been extensively studied in the past, but the current census of the stellar content is not complete yet and deserves further investigation. Aims: We take advantage of the second data release of the *Gaia* space mission to expand the census of stars in Chamaeleon and to revisit the properties of the stellar populations associated to the Chamaeleon I (Cha I) and Chamaeleon II (Cha II) dark clouds. Methods: We perform a membership analysis of the sources in the *Gaia* catalogue over a field of 100 deg$^2$ encompassing the Chamaeleon clouds, and use this new census of cluster members to investigate the 6D structure of the complex. Results: We identify 188 and 41 high-probability members of the stellar populations in Cha I and Cha II, respectively, including 19 and 7 new members. Our sample covers the magnitude range from $G = 6$ to $G = 20$ mag in Cha I, and from $G = 12$ to $G = 18$ mag in Cha II. We confirm that the northern and southern subgroups of Cha I are located at different distances ($191.4^{+0.8}_{-0.8}$ pc and $186.7^{+1.0}_{-1.0}$ pc), but they exhibit the same space motion within the reported uncertainties. Cha II is located at a distance of $197.5^{+1.0}_{-0.9}$ pc and exhibits a space motion that is consistent with Cha I within the admittedly large uncertainties on the spatial velocities of the stars that come from radial velocity data. The median age of the stars derived from the Hertzsprung-Russell diagram (HRD) and stellar models is about 1-2 Myr, suggesting that they are somewhat younger than previously thought. We do not detect significant age differences between the Chamaeleon subgroups, but we show that Cha II exhibits a higher fraction of disc-bearing stars compared to Cha I.

## 11. ALMA chemical survey of disk-outflow sources in Taurus (ALMA-DOT) V: Sample, overview, and demography of disk molecular emission

**Antonio Garufi, Linda Podio, Claudio Codella, Davide Fedele, Eleonora Bianchi, Cecile Favre, Francesca Bacciotti, Cecilia Ceccarelli, Seyma Mercimek, Kazi Rygl, Richard Teague, Leonardo Testi** We present an overview of the ALMA chemical survey of disk-outflow sources in Taurus (ALMA-DOT), a campaign devoted to the characterization of the molecular emission from partly embedded, young stars. The project aims at better understanding the gaseous products that are delivered to planets by means of high-resolution maps of assorted lines probing disks at the time of the planet formation (less than 1 Myr). Nine different molecules are surveyed by our observations of six Class I/flat-spectrum sources. A series of accompanying articles analyze specific targets and molecules. Here we describe the sample and provide a general overview of the results, focusing on the spatial distribution, column densities, and abundance ratios of $H_2CO$, CS, and CN. The results of this work are a first step toward the characterization of the disk chemical evolution that need to be complemented by further observations of less exceptional disks and customized thermo-chemical modeling.

## 12. The Geometry and Dynamical Role of Stellar Wind Bubbles in Photoionised HII Regions

**Sam Geen, Rebekka Bieri, Joakim Rosdahl, Alex de Koter** Winds from young massive stars contribute a large amount of energy to their host molecular clouds. This has consequences for the dynamics and observable structure of star-forming clouds. In this paper, we present radiative magnetohydrodynamic simulations of turbulent molecular clouds that form individual stars of 30, 60 and 120 solar masses emitting winds and ultraviolet radiation following realistic stellar evolution tracks. We find that winds contribute to the total radial momentum carried by the expanding nebula around the star at 10% of the level of photoionisation feedback, and have only a small effect on the radial expansion of the nebula. Radiation pressure is largely negligible in the systems studied here. The 3D geometry and evolution of wind bubbles is highly aspherical and chaotic, characterised by fast-moving "chimneys" and thermally-driven "plumes". These plumes can sometimes become disconnected from the stellar source due to dense gas flows in the cloud. Our results compare favourably with the findings of relevant simulations, analytic models and observations in the literature while demonstrating the need for full 3D simulations including stellar winds. However, more targeted simulations are needed to better understand results from observational studies.

## 13. 3D dynamics of the Orion cloud complex – Discovery of coherent radial gas motions at the 100-pc scale

**Josefa E. Großschedl, João Alves, Stefan Meingast, Gabor Herbst-Kiss** We present the first study of the 3D dynamics of the gas in the entire southern Orion cloud complex. We used the parallaxes and proper motions of YSOs from Gaia DR2 as a proxy for gas distance and proper motion, and the gas radial velocities from archival CO data, to compute the space motions of the different star-forming clouds in the complex, including subregions in Orion A, Orion B, and two outlying cometary clouds. From the analysis of the clouds' orbits in space and time, we find that they were closest about 6 Myr ago and are moving radially away from roughly the same region in space. This coherent 100-pc scale radial motion supports a scenario where the entire complex is reacting to a major feedback event, which we name the Orion-BB (big blast) event. This event, which we tentatively associate with the recently discovered Orion X stellar population, shaped the distribution and kinematics of the gas we observe today, although it is unlikely to have been the sole major feedback event in the region. We argue that the dynamics of most of the YSOs carry the memory of the feedback-driven star formation history in Orion and that the majority of the young stars in this complex are a product of large-scale triggering, which can raise the star formation rate by at least an order of magnitude, as for the head of Orion A (the Integral Shape Filament). Our results imply that a feedback, compression, and triggering process lies at the genesis of the Orion Nebula Cluster and NGC2023/2024 in Orion B, thus confirming broadly the classical feedback-driven scenario proposed in Elmegreen & Lada (1977). The space motions of the well-known young compact clusters, $\sigma$ Orionis and NGC 1977, are consistent with this scenario. A momentum estimate suggests that the energy of a few to several supernovae is needed to power the coherent 3D gas motion we measure in this paper.

## 14. Simulating Star Clusters Across Cosmic Time: II. Escape Fraction of Ionizing Photons from Molecular Clouds

**Chong-Chong He, Massimo Ricotti, Sam Geen** We calculate the hydrogen and helium-ionizing radiation escaping star-forming molecular clouds, as a function of the star cluster mass and compactness, using a set of high-resolution radiation-magneto-hydrodynamic simulations of star formation in self-gravitating, turbulent molecular clouds. In these simulations, presented in He, Ricotti and Geen (2019), the formation of individual massive stars are well resolved, and their UV radiation feedback and lifetime on the main sequence are modeled self-consistently. We find that the escape fraction of ionizing radiation from molecular clouds, $\langle f_{\rm esc}^{\rm MC}\rangle$, decreases with increasing mass of the star cluster and with decreasing compactness. Molecular clouds with densities typically found in the local Universe have negligible $\langle f_{\rm esc}^{\rm MC}\rangle$, ranging between 0.5% to 5%. Ten times denser molecular clouds have $\langle f_{\rm esc}^{\rm MC}\rangle \approx 10\% - 20\%$, while 100$\times$ denser clouds, which produce globular cluster progenitors, have $\langle f_{\rm esc}^{\rm MC}\rangle \approx 20\% - 60\%$. We find that $\langle f_{\rm esc}^{\rm MC}\rangle$ increases with decreasing gas metallicity, even when ignoring dust extinction, due to stronger radiation feedback. However, the total number of escaping ionizing photons decreases with decreasing metallicity because the star formation efficiency is reduced. We conclude that the sources of reionization at $z > 6$ must have been very compact star clusters forming in molecular clouds about 100$\times$ denser than in today's Universe, which leads to a significant production of old globular clusters progenitors.

## 15. Water maser variability in a high-mass YSO outburst – VERA and ALMA observations of S255 NIRS 3

**Tomoya Hirota, Riccardo Cesaroni, Luca Moscadelli, Koichiro Sugiyama, Ross A. Burns, Jungha Kim, Kazuyoshi Sunada, Yoshinori Yonekura** We carried out observations of the 22 GHz H2O masers in a high-mass protostar S255 NIRS 3 by using VERA. We measured the proper motions of the 22 GHz H2O masers associated with a bipolar outflow. The expansion velocity of the blueshifted bow shock traced by the 22 GHz H2O masers was 28 km s-1 corresponding to a dynamical timescale of 60 years. The direction of the maser outflow is slightly tilted compared with the radio jet, which could suggest a more recent ejection episode during the accretion burst event. The total flux density of the 22 GHz H2O masers has gradually increased from early 2017 and has become almost constant in 2018. For the first time, we reveal extended H2O maser emission at 22 GHz in a star forming region, which is partly resolved out by VERA and even by the most extended VLA configurations. We find that the flux variation of such an extended component is similar to that of the unresolved maser emission. We also conducted observations of the submillimeter continuum and the 321 GHz H2O masers with ALMA at Band 7. The continuum emission does not show significant variations compared with the previous observations performed 5 months before. We mapped the 321 GHz H2O masers in S255 NIRS 3 providing the fourth example, for this maser, of the spatial distribution in a high-mass star-forming region. The lower ratio of the 22 GHz/321 GHz maser luminosity in the blueshifted bow shock suggests a temperature (>1000 K), higher than for the other maser features in this region. We conclude that the bow shock structure traced by the 22 GHz H2O maser features is unlikely to be originating at the interface between the radio jet powered by the recent accretion outburst and the surrounding medium. The brightening of the 22 GHz H2O masers could be due to radiative excitation by photons form the infrared outburst escaping along the cavity created by the newly ejected material.

## 16. Rotating filament in Orion B: Do cores inherit their angular momentum from their parent filament?

**Cheng-Han Hsieh, Héctor G. Arce, Diego Mardones, Shuo Kong, Adele Plunkett** Angular momentum is one of the most important physical quantities that govern star formation. The initial angular momentum of a core may be responsible for its fragmentation and can have an influence on the size of the protoplanetary disk. To understand how cores obtain their initial angular momentum, it is important to study the angular momentum of filaments where they form. While theoretical studies on filament rotation have been explored, there exist very few observational measurements of the specific angular momentum in star-forming filaments. We present high-resolution N2D+ ALMA observations of the LBS 23 (HH24-HH26) region in Orion B, which provide one of the most reliable measurements of the specific angular momentum in a star-forming filament. We find the total specific angular momentum ($4 \times 10^{20} cm^2 s^{-1}$), the dependence of the specific angular momentum with radius (j(r) $\propto r^{1.83}$), and the ratio of rotational energy to gravitational energy ($\beta_{rot} \sim 0.04$) comparable to those observed in rotating cores with sizes similar to our filament width ($\sim$ 0.04 pc) in other star-forming regions. Our filament angular momentum profile is consistent with rotation acquired from ambient turbulence and with simulations that show cores and their host filaments develop simultaneously due to the multi-scale growth of nonlinear perturbation generated by turbulence.

## 17. A search for radio jets from massive young stellar objects. Association of radio jets with H2O and CH3OH masers

**U. Kavak, A. Sanchez-Monge, A. Lopez-Sepulcre, R. Cesaroni, F. F. S. van der Tak, L. Moscadelli, M. T. Beltran, P. Schilke** Recent theoretical and observational studies debate the similarities between the formation process of high-mass (>8 Msun) and low-mass stars. The formation of low-mass star formation is directly associated with the presence of disks and jets. According to this scenario, radio jets are expected to be common in high-mass star-forming regions. We aim to increase the number of known radio jets in high-mass star forming regions by searching for radio jet candidates at radio continuum wavelengths. We have used the Karl G. Jansky Very Large Array (VLA) to observe 18 high-mass star-forming regions in the C band (6 cm, 1.0 arcsec resolution) and K band (1.3 cm, 0.3 arcsec resolution). We have searched for radio jet candidates by studying the association of radio continuum sources with shock activity signposts. We have identified 7 as the most probable radio jets. The radio luminosity of the radio jet candidates is correlated with the bolometric luminosity and the outflow momentum rate. About 7-36% of the radio jet candidates are associated with non-thermal emission. The radio jet candidates associated with 6.7 GHz CH3OH maser emission are preferentially thermal winds and jets, while a considerable fraction of radio jet candidates associated with H2O masers show non-thermal emission, likely due to strong shocks. Our sample of 18 regions is divided in 8 less evolved, infrared-dark regions and 10 more evolved, infrared-bright regions. We have found that $\sim$ 71% of the identified radio jet candidates are located in the more evolved regions. Similarly, 25most probable radio jets, while up to 50one of these radio jet candidates. This suggests that the detection of radio jets in high-mass star forming regions is larger in slightly more evolved regions.

## 18. Interactions of a shock with a molecular cloud at various stages of its evolution due to thermal instability and gravity

**M. M. Kupilas, C. J. Wareing, J. M. Pittard, S. A. E. G. Falle** Using the adaptive mesh refinement code MG, we perform hydrodynamic simulations of the interaction of a shock with a molecular cloud evolving due to thermal instability and gravity. To explore the relative importance of these processes, three case studies are presented. The first follows the formation of a molecular cloud out of an initially quiescent atomic medium due to the effects of thermal instability and gravity. The second case introduces a shock whilst the cloud is still in the warm atomic phase, and the third scenario introduces a shock once the molecular cloud has formed. The shocks accelerate the global collapse of the clouds with both experiencing local gravitational collapse prior to this. When the cloud is still atomic, the evolution is shock dominated and structures form due to dynamical instabilities within a radiatively cooled shell. While the transmitted shock can potentially trigger the thermal instability, this is prevented as material is shocked multiple times on the order of a cloud crushing time-scale. When the cloud is molecular, the post-shock flow is directed via the pre-existing structure through low-density regions in the inter-clump medium. The clumps are accelerated and deformed as the flow induces clump-clump collisions and mergers that collapse under gravity. For a limited period, both shocked cases show a mixture of Kolmogorov and Burgers turbulence-like velocity and logarithmic density power spectra, and strongly varying density spectra. The clouds presented in this work provide realistic conditions that will be used in future feedback studies.

## 19. Viscous Heating and Boundary Layer Accretion in the Disk of Outbursting Star FU Orionis

**Aaron Labdon, Stefan Kraus, Claire L Davies, Alexander Kreplin, John D Monnier, Jean-Baptiste Le Bouquin, Narsireddy Anugu, Theo Brummelaar, Benjamin Setterholm, Tyler Gardener, Jacob Ennis, Cyprien Lanthermann, Gail Schaefer, Anna Laws** Context. FU Orionis is the archetypal FUor star, a subclass of young stellar object (YSO) that undergo rapid brightening events, often gaining 4-6 magnitudes on timescales of days. This brightening is often associated with a massive increase in accretion; one of the most ubiquitous processes in astrophysics from planets and stars to super-massive black holes. We present multi-band interferometric observations of the FU Ori circumstellar environment, including the first J-band interferometric observations of a YSO. Aims. We investigate the morphology and temperature gradient of the inner-most regions of the accretion disk around FU Orionis. We aim to characterise the heating mechanisms of the disk and comment on potential outburst triggering processes. Methods. Recent upgrades to the MIRC-X instrument at the CHARA array allowed the first dual-band J and H observations of YSOs.Using baselines up to 331 m, we present high angular resolution data of a YSO covering the near-infrared bands J, H, and K. The unprecedented spectral range of the data allows us to apply temperature gradient models to the innermost regions of FU Ori. Results. We spatially resolve the innermost astronomical unit of the disk and determine the exponent of the temperature gradient of the inner disk to $T = r^{-0.74\pm0.02}$. This agrees with theoretical work that predicts $T = r^{-0.75}$ for actively accreting, steady state disks, a value only obtainable through viscous heating within the disk. We find a disk which extends down to the stellar surface at $0.015 \pm 0.007$ au where the temperature is found to be $5800 \pm 700$ K indicating boundary layer accretion. We find a disk inclined at $32 \pm 4^\circ$ with a minor-axis position angle of $34 \pm 11^\circ$.

## 20. Chemically tracing the water snowline in protoplanetary disks with $HCO^+$

**M. Leemker, M. L. R. van 't Hoff, L. Trapman, M. L. van Gelder, M. R. Hogerheijde, D. Ruíz-Rodríguez, E. F. van Dishoeck** [Abridged] Planet formation is expected to be enhanced around snowlines in protoplanetary disks, in particular around the water snowline. However, the close proximity of the water snowline to the host star and water in the Earth's atmosphere makes a direct detection of the water snowline in protoplanetary disks challenging. Following earlier work on protostellar envelopes, the aim of this research is to investigate the validity of $HCO^+$ and $H^{13}CO^+$, as tracers of the water snowline in protoplanetary disks, as $HCO^+$ is destroyed by gas-phase water. Two small chemical networks are used to predict the $HCO^+$ abundance in a typical Herbig Ae disk. Subsequently, the corresponding emission profiles are modelled for $H^{13}CO^+$ and $HCO^+$ $J = 2-1$, which provides the best balance between brightness and optical depth effects of the continuum emission. The $HCO^+$ abundance jumps by two orders of magnitude just outside the water snowline at 4.5 AU. We find that the emission of $H^{13}CO^+$ and $HCO^+$ is ring-shaped due to three effects: destruction of $HCO^+$ by gas-phase water, continuum optical depth, and molecular excitation effects. The presence of gas-phase water causes an additional drop of only ∼13in the center of the disk, for $H^{13}CO^+$ and $HCO^+$, respectively. For the much more luminous outbursting source V883Ori, our models predict that the effect of dust and excitation are not limiting if the snowline is located outside ∼40 AU. Our analysis of ALMA observations of $HCO^+$ $J = 3-2$ is consistent with the water snowline located around 100 AU. The $HCO^+$ abundance drops steeply around the water snowline, but dust and excitation can conceal the drop in $HCO^+$ emission due to the water snowline. Therefore, locating the water snowline with $HCO^+$ in Herbig disks is very difficult, but it is possible for outbursting sources like V883Ori.

## 21. Inferring (Sub)millimeter Dust Opacities and Temperature Structure in Edge-on Protostellar Disks From Resolved Multi-Wavelength Continuum Observations: The Case of the HH 212 Disk

**Zhe-Yu Daniel Lin, Chin-Fei Lee, Zhi-Yun Li, John Tobin, Neal Turner** (Sub)millimeter dust opacities are required for converting the observable dust continuum emission to the mass, but their values have long been uncertain, especially in disks around young stellar objects. We propose a method to constrain the opacity $\kappa_\nu$ in edge-on disks from a characteristic optical depth $\tau_{0,\nu}$, the density $\rho_0$ and radius $R_0$ at the disk outer edge through $\kappa_\nu = \tau_{0,\nu}/(\rho_0 R_0)$ where $\tau_{0,\nu}$ is inferred from the shape of the observed flux along the major axis, $\rho_0$ from gravitational stability considerations, and $R_0$ from direct imaging. We applied the 1D semi-analytical model to the embedded, Class 0, HH 212 disk, which has high-resolution data in ALMA Band 9, 7, 6, and 3 and VLA Ka band ($\lambda$=0.43, 0.85, 1.3, 2.9, and 9.1 mm). The modeling of the HH 212 disk is extended to 2D through RADMC-3D radiative transfer calculations. We find a dust opacity of $\kappa_\nu \approx 1.9\times10^{-2}$, $1.3\times10^{-2}$, and $4.9\times10^{-3}$ cm$^2$ per gram of gas and dust for ALMA Bands 7, 6, and 3, respectively with uncertainties dependent on the adopted stellar mass. The inferred opacities lend support to the widely used prescription $\kappa_\lambda = 2.3\times10^{-2}(1.3\mathrm{mm}/\lambda)$ cm$^2$ g$^{-1}$ advocated by Beckwith et al. (1990). We inferred a temperature of 45K at the disk outer edge which increases radially inward. It is well above the sublimation temperatures of ices such as CO and $N_2$, which supports the notion that the disk chemistry cannot be completely inherited from the protostellar envelope.

## 22. ALMA View of the Infalling Envelope around a Massive Protostar in S255IR SMA1

**Sheng-Yuan Liu, Yu-Nung Su, Igor Zinchenko, Kuo-Song Wang, Dominique M. -A. Meyer, Yuan Wang, I-Ta Hsieh** The massive young stellar object S255IR NIRS3 embedded in the star forming core SMA1 has been recently observed with a luminosity burst, which is conjectured as a disc-mediated variable accretion event. In this context, it is imperative to characterize the gas properties around the massive young stellar object. With this in mind, we carried out high angular resolution observations with the Atacama Large Millimeter and submillimeter Array and imaged the 900 $\mu m$ dust continuum and the $CH_3CN$ $J$=19−18 $K$=0−10 transitions of S255IR SMA1. The integrated $CH_3CN$ emission exhibits an elongated feature with an extent of 1800 au in the northwest-southeast direction at a position angle of 165 degree, which is nearly perpendicular to the bipolar outflow. We confirm the presence of dense (a few $\times 10^9$ cm$^{-3}$) and hot ($\sim$ 400 K) gas immediately surrounding the central protostar. The $CH_3CN$ emission features a velocity gradient along the elongated ridge and by modelling the gas kinematics based on features in the position-velocity diagram, we infer that the gas is best described by a flattened rotating infalling envelope (or pseudo-disc). A mass infall rate of a few $\times$ $10^{-4}$ solar-mass per year is derived. If there exists a putative Keplerian disc directly involved in the mass accretion onto the star and jet/outflow launching, it is likely smaller than 125 au and unresolved by our observations. We show qualitative resemblances between the gas properties (such as density and kinematics) in 255IR SMA1 inferred from our observations and those in a numerical simulation particularly tailored for studying the burst mode of massive star formation.

## 23. Discovery of a mid-infrared protostellar outburst of exceptional amplitude

**P. W. Lucas, J. Elias, S. Points, Z. Guo, L. C. Smith, B. Stecklum, E. Vorobyov, C. Morris, J. Borissova, R. Kurtev, C. Contreras Pena, N. Medina, D. Minniti, V. D. Ivanov, R. K. Saito** We report the discovery of a mid-infrared outburst in a Young Stellar Object (YSO) with an amplitude close to 8 mag at $\lambda$≈4.6 $\mu$m. WISEA J142238.82-611553.7 is one of 23 highly variable WISE sources discovered in a search of Infrared Dark Clouds (IRDCs). It lies within the small IRDC G313.671-0.309 (d≈2.6 kpc), seen by the Herschel/HiGal survey as a compact, massive cloud core that may have been measurably warmed by the event. Pre-outburst data from Spitzer in 2004 suggest that it is a class I YSO, a view supported by observation of weak 2.12 $\mu$m $H_2$ emission in an otherwise featureless red continuum spectrum taken in 2019 (6 mag below the peak in $K_s$). Spitzer, WISE and VVV data indicate that the outburst began by 2006 and has a duration >13 yr, with a fairly flat peak from 2010–2014. The outburst luminosity of a few $\times 10^2$ Lsun is consistent with an accretion rate Mdot ≈ $10^{-4}$ Msun/yr, comparable to a classical FU Orionis event. The 4.6 $\mu$m peak in 2010 implies T = 800-1000 K and a disc radial location R≈4.5 au for the emitting region. The colour evolution suggests subsequent progression outward. The apparent absence of the hotter matter expected in thermal instability or MRI models may be due to complete obscuration of the innermost disc, e.g. by an edge-on disc view. Alternatively, disc fragmentation/infalling fragment models might more naturally explain a mid-infrared peak, though this is not yet clear.

## 24. Extended stellar systems in the solar neighborhood – V. Discovery of coronae of nearby star clusters

**Stefan Meingast, João Alves, Alena Rottensteiner** In this paper, we present a novel view on the morphology and the dynamical state of 10 prominent, nearby ($\leq$ 500 pc), and young (∼30-300 Myr) open star clusters with Gaia DR2: $\alpha$ Per, Blanco 1, IC 2602, IC 2391, Messier 39, NGC 2451A, NGC 2516, NGC 2547, Platais 9, and the Pleiades. We introduce a pioneering member identification method that is informed by cluster bulk velocities and deconvolves the spatial distribution with a mixture of Gaussians. Our approach enables inferring the clusters' true spatial distribution by effectively filtering field star contaminants while at the same time mitigating the impact of positional errors along the line of sight. This first application of the method reveals the existence of vast stellar coronae, extending for $\gtrsim$100 pc and surrounding the, by comparison tiny and compact, cluster cores. The coronae and cores form intertwined, co-eval, and co-moving extended cluster populations, each encompassing tens of thousands of cubic parsec and stretching across tens of degrees on the sky. Our analysis shows that the coronae are gravitationally unbound but largely comprise the bulk of the populations' stellar mass. Most systems are in a highly dynamic state, showing evidence of expansion and sometimes simultaneous contraction along different spatial axes. The velocity field of the extended populations for the cluster cores appears asymmetric but is aligned along a spatial axis unique to each cluster. The overall spatial distribution and the kinematic signature of the populations are largely consistent with the differential rotation pattern of the Milky Way. This finding underlines the important role of global Galactic dynamics to the fate of stellar systems. Our results highlight the complexity of the Milky Way's open cluster population and call for a new perspective on the characterization and dynamical state of open clusters.

## 25. High-Resolution Mid-Infrared Spectroscopy of GV Tau N: Surface Accretion and Detection of Ammonia in a Young Protoplanetary Disk

**Joan R. Najita, John S. Carr, Sean D. Brittain, John H. Lacy, Matthew J. Richter, Greg W. Doppmann** Physical processes that redistribute or remove angular momentum from protoplanetary disks can drive mass accretion onto the star and affect the outcome of planet formation. Despite ubiquitous evidence that protoplanetary disks are engaged in accretion, the

process(es) responsible remain unclear. Here we present evidence for redshifted molecular absorption in the spectrum of a Class I source that indicates rapid inflow at the disk surface. High resolution mid-infrared spectroscopy of GV Tau N reveals a rich absorption spectrum of individual lines of C2H2, HCN, NH3, and water. From the properties of the molecular absorption, we can infer that it carries a significant accretion rate ( 1e-8 to 1e-7 Msun/yr), comparable to the stellar accretion rates of active T Tauri stars. Thus we may be observing disk accretion in action. The results may provide observational evidence for supersonic "surface accretion flows," which have been found in MHD simulations of magnetized disks. The observed spectra also represent the first detection of ammonia in the planet formation region of a protoplanetary disk. With ammonia only comparable in abundance to HCN, it cannot be a major missing reservoir of nitrogen. If, as expected, the dominant nitrogen reservoir in inner disks is instead N2, its high volatility would make it difficult to incorporate into forming planets, which may help to explain the low nitrogen content of the bulk Earth.

## 26. Observations of magnetic fields surrounding LkH$\alpha$ 101 taken by the BISTRO survey with JCMT-POL-2

**BISTRO Collaboration, Nguyen Bich Ngoc et al.** We report the first high spatial resolution measurement of magnetic fields surrounding LkH$\alpha$ 101, a part of the Auriga-California molecular cloud. The observations were taken with the POL-2 polarimeter on the James Clerk Maxwell Telescope within the framework of the B-fields In Star-forming Region Observations (BISTRO) survey. Observed polarization of thermal dust emission at 850 $\mu$m is found to be mostly associated with the red-shifted gas component of the cloud. The magnetic field displays a relatively complex morphology. Two variants of the Davis-Chandrasekhar-Fermi method, unsharp masking and structure function, are used to calculate the strength of magnetic fields in the plane of the sky, yielding a similar result of $B_{\rm POS} \sim 115$ $\mu$G. The mass-to-magnetic-flux ratio in critical value units, $\lambda \sim 0.3$, is the smallest among the values obtained for other regions surveyed by POL-2. This implies that the LkH$\alpha$ 101 region is sub-critical and the magnetic field is strong enough to prevent gravitational collapse. The inferred $\delta B/B_0 \sim 0.3$ implies that the large scale component of the magnetic field dominates the turbulent one. The variation of the polarization fraction with total emission intensity can be fitted by a power-law with an index of $\alpha = 0.82 \pm 0.03$, which lies in the range previously reported for molecular clouds. We find that the polarization fraction decreases rapidly with proximity to the only early B star (LkH$\alpha$ 101) in the region. The magnetic field tangling and the joint effect of grain alignment and rotational disruption by radiative torques are potential of explaining such a decreasing trend.

## 27. Deciphering the 3-D Orion Nebula-II: A low-ionization region of multiple velocity components southwest of Theta1OriC confounds interpretation of low velocity resolution studies of temperature, density, and abundance

**C. R. O'Dell, N. P. Abel, G. J. Ferland** We establish that there are two velocity systems along lines-of-sight that contribute to the emission-line spectrum of the the brightest parts of the Orion Nebula. These overlie the Orion-S embedded molecular cloud southwest of the dominant ionizing star (Theta1OriC). Examination of 10x10" samples of high spectral resolution emission-line spectra of this region reveals it to be of low ionization, with velocities and ionization different from the central part of the Nebula. These properties jeopardize earlier determinations of abundance and physical conditions since they indicate that this region is much more complex than has been assumed in analyzing earlier spectroscopic studies and argue for use of very high spectral resolution or known simple regions in future studies.

## 28. Ring formation by coagulation of dust aggregates in early phase of disk evolution around a protostar

**Satoshi Ohashi, Hiroshi Kobayashi, Riouhei Nakatani, Satoshi Okuzumi, Hidekazu Tanaka, Koji Murakawa, Yichen Zhang, Hauyu Baobab Liu, Nami Sakai** Ring structures are observed by (sub-)millimeter dust continuum emission in various circumstellar disks from early stages of Class 0 and I to late stage of Class II young stellar objects (YSOs). In this paper, we study one of the possible scenarios of such ring formation in early stage, which is coagulation of dust aggregates. The dust grains grow in an inside-out manner because the growth timescale is roughly proportional to the orbital period. The boundary of the dust evolution can be regarded as the growth front, where the growth time is comparable to the disk age. With radiative transfer calculations based on the dust coagulation model, we find that the growth front can be observed as a ring structure because dust surface density is sharply changed at this position. Furthermore, we confirm that the observed ring positions in the YSOs with an age of $\lesssim 1$ Myr are consistent with the growth front. The growth front could be important to create the ring structure in particular for early stage of the disk evolution such as Class 0 and I sources.

## 29. Substructures in the Disk-Forming Region of the Class 0 Low-Mass Protostellar Source IRAS 16293-2422 Source A on a 10 au Scale

**Yoko Oya, Satoshi Yamamoto** We have observed the Class 0 protostellar source IRAS 16293-2422 A in the C17O and H2CS lines as well as the 1.3 mm dust continuum with the Atacama Large Millimeter/submillimeter Array at an angular resolution

of 0."1 (14 au). The continuum emission of the binary component, Source A, reveals the substructure consisting of 5 intensity peaks within 100 au from the protostar. The C17O emission mainly traces the circummultiple structure on a 300 au scale centered at the intensity centroid of the continuum, while it is very weak within the radius of 50 au from the centroid. The H2CS emission, in contrast, traces the rotating disk structure around one of the continuum peaks (A1). Thus, it seems that the rotation centroid of the circummultiple structure is slightly different from that of the disk around A1. We derive the rotation temperature by using the multiple lines of H2CS. As approaching to the protostar A1, the rotation temperature steeply rises up to 300 K or higher at the radius of 50 au from the protostar. It is likely due to a local accretion shock and/or the preferential protostellar heating of the transition zone from the circummultiple structure to the disk around A1. This position corresponds to the place where the organic molecular lines are reported to be enhanced. Since the rise of the rotation temperature of H2CS most likely represents the rise of the gas and dust temperatures, it would be related to the chemical characteristics of this prototypical hot corino.

## 30. JCMT POL-2 and BISTRO Survey observations of magnetic fields in the L1689 molecular cloud

**Kate Pattle, Shih-Ping Lai, James Di Francesco, Sarah Sadavoy, Derek Ward-Thompson, Doug Johnstone, Thiem Hoang, Doris Arzoumanian, Pierre Bastien, Tyler L. Bourke, Simon Coudé, Yasuo Doi, Chakali Eswaraiah, Lapo Fanciullo, Ray S. Furuya, Jihye Hwang, Charles L. H. Hull, Jihyun Kang, Kee-Tae Kim, Florian Kirchschlager, Jungmi Kwon, Woojin Kwon, Chang Won Lee, Tie Liu, Matt Redman, Archana Soam, Mehrnoosh Tahani, Motohide Tamura, Xindi Tang** We present 850$\mu$m polarization observations of the L1689 molecular cloud, part of the nearby Ophiuchus molecular cloud complex, taken with the POL-2 polarimeter on the James Clerk Maxwell Telescope (JCMT). We observe three regions of L1689: the clump L1689N which houses the IRAS 16293-2422 protostellar system, the starless clump SMM-16, and the starless core L1689B. We use the Davis-Chandrasekhar-Fermi method to estimate plane-of-sky field strengths of $366 \pm 55$ $\mu$G in L1689N, $284 \pm 34$ $\mu$G in SMM-16, and $72 \pm 33$ $\mu$G in L1689B, for our fiducial value of dust opacity. These values indicate that all three regions are likely to be magnetically trans-critical with sub-Alfvénic turbulence. In all three regions, the inferred mean magnetic field direction is approximately perpendicular to the local filament direction identified in *Herschel* Space Telescope observations. The core-scale field morphologies for L1689N and L1689B are consistent with the cloud-scale field morphology measured by the *Planck* Space Observatory, suggesting that material can flow freely from large to small scales for these sources. Based on these magnetic field measurements, we posit that accretion from the cloud onto L1689N and L1689B may be magnetically regulated. However, in SMM-16, the clump-scale field is nearly perpendicular to the field seen on cloud scales by *Planck*, suggesting that it may be unable to efficiently accrete further material from its surroundings.

## 31. Growing and Trapping Pebbles with Fragile Collisions of Particles in Protoplanetary Disks

**Paola Pinilla, Christian T. Lenz, Sebastian M. Stammler** [abridged] Recent laboratory experiments indicate that destructive collisions of icy dust particles occur with much lower velocities than previously thought. When these new velocities are considered from laboratory experiments in dust evolution models, a growth to pebble sizes in protoplanetary disks (PPDs) is difficult. This may contradict (sub-)mm observations and challenge the formation of planetesimals and planets. We investigate the conditions that are required in dust evolution models for growing and trapping pebbles in PPDs when the fragmentation speed is $1\mathrm{ms}^{-1}$ in the entire disk. We distinguish the parameters controlling the effects of turbulent velocities, vertical stirring, radial diffusion, and gas viscous evolution, always assuming that particles cannot diffuse faster (radially or vertically) than the gas. To form pebbles and produce effective particle trapping, the parameter that controls the particle turbulent velocities must be small ($\delta_t \lesssim 10^{-4}$). In these cases, the vertical settling can limit the formation of pebbles, which also prevents particle trapping. Therefore the parameter that sets the vertical settling of the grains must be $\delta_z < 10^{-3}$. Our results suggest that different combinations of the particle and gas diffusion parameters can lead to a large diversity of millimeter fluxes and dust-disk radii. When pebble formation occurs and trapping is efficient, gaps and rings have higher contrast at mm-emission than in the NIR. In the case of inefficient trapping, structures are also formed at the two wavelengths, producing deeper and wider gaps in the NIR. Our results highlight the importance of obtaining observational constraints of gas and particle diffusion parameters and the properties of gaps at short and long wavelengths to better understand basic features of PPDs and the origin of the structures that are observed in these objects.

## 32. Observational constraints on the likelihood of $^{26}$Al in planet-forming environments

**Megan Reiter** Recent work suggests that $^{26}$Al may determine the water budget in terrestrial exoplanets as its radioactive decay dehydrates planetesimals leading to rockier compositions. Here I consider the observed distribution of $^{26}$Al in the Galaxy and typical star-forming environments to estimate the likelihood of $^{26}$Al enrichment during planet formation. I do not assume Solar-System-specific constraints as I am interested in enrichment for exoplanets generally. Observations indicate that high-mass stars dominate the production of $^{26}$Al with nearly equal contributions from their winds and supernovae. $^{26}$Al abundances

are comparable to those in the early Solar System in the high-mass star-forming regions where most stars (and thereby most planets) form. These high abundances appear to be maintained for a few Myr, much longer than the 0.7 Myr half-life. Observed bulk $^{26}$Al velocities are an order of magnitude slower than expected from winds and supernovae. These observations are at odds with typical model assumptions that $^{26}$Al is provided instantaneously by high velocity mass loss from supernovae and winds. Regular replenishment of $^{26}$Al especially when coupled with the small age differences that are common in high-mass star-forming complexes, may significantly increase the number of star/planet-forming systems exposed to $^{26}$Al. Exposure does not imply enrichment, but the order of magnitude slower velocity of $^{26}$Al may alter the fraction that is incorporated into planet-forming material. Together, this suggests that the conditions for rocky planet formation are not rare, nor are they ubiquitous, as small regions like Taurus that lack high-mass stars to produce $^{26}$Al may be less likely to form rocky planets. I conclude with suggested directions for future studies.

## 33. Kinematic Analysis of a Protostellar Multiple System: Measuring the Protostar Masses and Assessing Gravitational Instability in the Disks of L1448 IRS3B and L1448 IRS3A

**Nickalas K. Reynolds, John J. Tobin, Patrick D. Sheehan, Sarah I. Sadavoy, Kaitlin M. Kratter, Zhi-Yun Li, Claire J. Chandler, Dominique M. Segura-Cox, Leslie W. Looney, Michael M. Dunham** We present new Atacama Large Millimeter/submillimeter Array (ALMA) observations towards a compact (230 au separation) triple protostar system, L1448 IRS3B, at 879$\mu$ with 0.11 $\times$ 0.05 arcsec resolution. Spiral arm structure within the circum-multiple disk is well resolved in dust continuum toward IRS3B, and we detect the known wide (2300 au) companion, IRS3A, also resolving possible spiral substructure. Using dense gas tracers, C17O, H13CO+, and H13CN, we resolve the Keplerian rotation for both the circum-triple disk in IRS3B and the disk around IRS3A. Furthermore, we use the molecular line kinematic data and radiative transfer modeling of the molecular line emission to confirm that the disks are in Keplerian rotation with fitted masses of $1.19^{+0.13}_{-0.07}$ for IRS3B-ab, $1.51^{+0.06}_{-0.07}$ Msun for IRS3A, and place an upper limit on the central protostar mass for the tertiary IRS3B-c of 0.2 Msun. We measure the mass of the fragmenting disk of IRS3B to be 0.29 Msun from the dust continuum emission of the circum-multiple disk and estimate the mass of the clump surrounding IRS3B-c to be 0.07 Msun. We also find that the disk around IRS3A has a mass of 0.04 Msun. By analyzing the Toomre Q parameter, we find the IRS3A circumstellar disk is gravitationally stable (Q>5), while the IRS3B disk is consistent with a gravitationally unstable disk (Q<1) between the radii 200-500 au. This coincides with the location of the spiral arms and the tertiary companion IRS3B-c, supporting the hypothesis that IRS3B-c was formed in situ via fragmentation of a gravitationally unstable disk.

## 34. Accretion and outflow activity in proto-brown dwarfs

**B. Riaz, J. Bally** We present a near-infrared study of accretion and outflow activity in 6 Class 0/I proto-brown dwarfs (proto-BDs) using VLT/SINFONI spectroscopy and spectro-imaging observations. The spectra show emission in several [FeII] and $H_2$ lines associated with jet/outflow activity, and in the accretion diagnostics of Pa$\beta$ and Br$\gamma$ lines. The peak velocities of the [FeII] lines (>100 km s$^{-1}$) are higher than the $H_2$ lines. The Class 0 proto-BDs show strong emission in the $H_2$ lines but the [FeII] lines are undetected, while the Class I objects show emission in both [FeII] and $H_2$ lines, suggesting an evolutionary trend in the jets from a molecular to an ionic composition. Extended emission with knots is seen in the [FeII] and $H_2$ spectro-images for 3 proto-BDs, while the rest show compact morphologies with a peak on-source. The accretion rates for the proto-BDs span the range of ($2\times10^{-6}$ – $2\times10^{-8}$) Msun yr$^{-1}$, while the mass loss rates are in the range of ($4\times10^{-8}$ – $5\times10^{-9}$) Msun yr$^{-1}$. These rates are within the range measured for low-mass protostars and higher than Class II brown dwarfs. We find a similar range in the jet efficiency for proto-BDs as measured in protostars. We have performed a study of the Brackett decrement from the Br7-Br19 lines detected in the proto-BDs. The upper Brackett lines of Br13-Br19 are only detected in the earlier stage systems. The ratios of the different Brackett lines with respect to the Br$\gamma$ line intensity are consistent with the ratios expected from Case B recombination.

## 35. Survey of ortho-$H_2D^+$ in high-mass star-forming regions

**G. Sabatini, S. Bovino, A. Giannetti, F. Wyrowski, M. A. Órdenes, R. Pascale, T. Pillai, M. Wienen, T. Csengeri, K. M. Menten** (Abridged) We present a large sample of o-$H_2D^+$ observations in high-mass star-forming regions and discuss possible empirical correlations with relevant physical quantities to assess its role as a chronometer of star-forming regions through different evolutionary stages. APEX observations of the ground-state transition of o-$H_2D^+$ were analysed in a sample of massive clumps selected from ATLASGAL at different evolutionary stages. Column densities and beam-averaged abundances of o-$H_2D^+$ with respect to $H_2$, $X$(o-$H_2D^+$), were obtained by modelling the spectra under the assumption of local thermodynamic equilibrium. We detect 16 sources in o-$H_2D^+$ and find clear correlations between $X$(o-$H_2D^+$) and the clump bolometric luminosity and the dust temperature, while only a mild correlation is found with the CO-depletion factor. In addition, we see a clear correlation with the luminosity-to-mass ratio, which is known to trace the evolution of the star formation process. This would indicate that the deuterated forms of $H_3^+$ are more abundant in the early stages of the star formation process and that deuteration is influenced by the time evolution of the clumps. In this respect, our findings would suggest that the $X$(o-$H_2D^+$) abundance is mainly affected by the thermal changes rather than density changes in the gas. We

have employed these findings together with observations of $H^{13}CO^+$, $DCO^+$, and $C^{17}O$ to provide an estimate of the cosmic-ray ionisation rate in a sub-sample of eight clumps based on recent analytical work. Our study presents the largest sample of o-$H_2D^+$ in star-forming regions to date. The results confirm that the deuteration process is strongly affected by temperature and suggests that o-$H_2D^+$ can be considered a reliable chemical clock during the star formation processes, as proved by its strong temporal dependence.

## 36. The TW Hya Rosetta Stone Project II: Spatially resolved emission of formaldehyde hints at low-temperature gas-phase formation

**Jeroen Terwisscha van Scheltinga, Michiel R. Hogerheijde, L. Ilsedore Cleeves, Ryan A. Loomis, Catherine Walsh, Karin I. Öberg, Edwin A. Bergin, Jennifer B. Bergner, Geoffrey A. Blake, Jenny K. Calahan, Paolo Cazzoletti, Ewine F. van Dishoeck, Viviana V. Guzmán, Jane Huang, Mihkel Kama, Chunhua Qi, Richard Teague, David J. Wilner** Formaldehyde ($H_2CO$) is an important precursor to organics like methanol ($CH_3OH$). It is important to understand the conditions that produce $H_2CO$ and prebiotic molecules during star and planet formation. $H_2CO$ possesses both gas-phase and solid-state formation pathways, involving either UV-produced radical precursors or CO ice and cold ($\lesssim 20$ K) dust grains. To understand which pathway dominates, gaseous $H_2CO$'s ortho-to-para ratio (OPR) has been used as a probe, with a value of 3 indicating "warm" conditions and $< 3$ linked to cold formation in the solid-state. We present spatially resolved ALMA observations of multiple ortho- and para-$H_2CO$ transitions in the TW Hya protoplanetary disk to test $H_2CO$ formation theories during planet formation. We find disk-averaged rotational temperatures and column densities of $33 \pm 2$ K, $(1.1 \pm 0.1) \times 10^{12}$ cm$^{-2}$ and $25 \pm 2$ K, $(4.4 \pm 0.3) \times 10^{11}$ cm$^{-2}$ for ortho- and para-$H_2CO$, respectively, and an OPR of $2.49 \pm 0.23$. A radially resolved analysis shows that the observed $H_2CO$ emits mostly at rotational temperatures of 30-40 K, corresponding to a layer with $z/R \geq 0.25$. The OPR is consistent with 3 within 60 au, the extent of the pebble disk, and decreases beyond 60 au to $2.0 \pm 0.5$. The latter corresponds to a spin temperature of 12 K, well below the rotational temperature. The combination of relatively uniform emitting conditions, a radial gradient in the OPR, and recent laboratory experiments and theory on OPR ratios after sublimation, lead us to speculate that gas-phase formation is responsible for the observed $H_2CO$ across the TW Hya disk.

## 37. The SEDIGISM survey: first data release and overview of the Galactic structure

**SEDIGISM Collaboration, F. Schuller et al.** The SEDIGISM (Structure, Excitation and Dynamics of the Inner Galactic Interstellar Medium) survey used the APEX telescope to map 84 deg$^2$ of the Galactic plane between l = -60 deg and l = +31 deg in several molecular transitions, including 13CO(2-1) and C18O(2-1), thus probing the moderately dense ($\sim 10^3$ cm$^-3$) component of the interstellar medium. With an angular resolution of 30" and a typical 1-sigma sensitivity of 0.8-1.0 K at 0.25 km/s velocity resolution, it gives access to a wide range of structures, from individual star-forming clumps to giant molecular clouds and complexes. The coverage includes a good fraction of the first and fourth Galactic quadrants, allowing us to constrain the large scale distribution of cold molecular gas in the inner Galaxy. In this paper we provide an updated overview of the full survey and the data reduction procedures used. We also assess the quality of these data and describe the data products that are being made publicly available as part of this first data release (DR1). We present integrated maps and position-velocity maps of the molecular gas and use these to investigate the correlation between the molecular gas and the large scale structural features of the Milky Way such as the spiral arms, Galactic bar and Galactic centre. We find that approximately 60 per cent of the molecular gas is associated with the spiral arms and these appear as strong intensity peaks in the derived Galactocentric distribution. We also find strong peaks in intensity at specific longitudes that correspond to the Galactic centre and well known star forming complexes, revealing that the 13CO emission is concentrated in a small number of complexes rather than evenly distributed along spiral arms.

## 38. From parallel to perpendicular – On the orientation of magnetic fields in molecular clouds

**D. Seifried, S. Walch, M. Weis, S. Reissl, J. D. Soler, R. S. Klessen, P. R. Joshi** We present synthetic dust polarization maps of simulated molecular clouds (MCs) with the goal to systematically explore the origin of the relative orientation of the magnetic field (**B**) with respect to the MC sub-structures identified in density ($n$; 3D) and column density ($N$; 2D). The polarization maps are generated with the radiative transfer code POLARIS, including self-consistently calculated efficiencies for radiative torque alignment. The MCs are formed in two sets of 3D MHD simulations: in (i) colliding flows (CF), and (ii) the SILCC-Zoom simulations. In 3D, for the CF simulations with an initial field strength below $\sim$5 $\mu$G, **B** is oriented parallel or randomly with respect to the $n$-structures. For CF runs with stronger initial fields and all SILCC-Zoom simulations, which have an initial field strength of 3 $\mu$G, a flip from parallel to perpendicular orientation occurs at high densities of $n_{\rm trans} \simeq 10^2$ - $10^3$ cm$^{-3}$. We suggest that this flip happens if the MC's mass-to-flux ratio, $\mu$, is close to or below the critical value of 1. This corresponds to a field strength around 3 - 5 $\mu$G. In 2D, we use the Projected Rayleigh Statistics (PRS) to study the orientation of **B**. If present, the flip in orientation occurs at $N_{\rm trans} \simeq 10^{21-21.5}$ cm$^{-2}$, similar to the observed transition value from sub- to supercritical magnetic fields in the ISM. However, projection effects can reduce the power of the PRS method: Depending on

the MC or LOS, the projected maps of the SILCC-Zoom simulations do not always show the flip, although expected from the 3D morphology. Such projection effects can explain the variety of recently observed field configurations, in particular within a single MC. Finally, we do not find a correlation between the observed orientation of **B** and the $N$-PDF.

## 39. Atlas of CO-Line Shells and Cavities around Galactic Supernova Remnants with FUGIN

**Yoshiaki Sofue, Mikito Kohno, Tomofumi Umemoto** A morphological search for molecular shells and cavities was performed around 63 Galactic supernova remnants (SNR) at $10^\circ \leq l \leq 50^\circ$, $|b| \leq 1^\circ$using the FUGIN (FOREST Unbiased Galactic Imaging survey with the Nobeyama 45-m telescope) CO line data at high angular ($20''$) and velocity (1.3 km s$^{-1}$) resolutions. The results are presented as supplementary data for general purpose for investigations of the interaction between SNRs and interstellar matter in the form of an atlas of CO-line maps superposed on radio continuum maps at 20 cm along with a list of their kinematic distances determined from CO-line radial velocities. (Full atlas including all figures is available in this URL: https://nro-fugin.github.io/2020-apjs-CO-Shell-Atlas-SNR-FUGIN-IX.pdf)

## 40. An ALMA view of the Galactic super star cluster RCW38 at 270-AU resolution

**Kazufumi Torii, Kazuki Tokuda, Kengo Tachihara, Toshikazu Onishi, Yasuo Fukui** We report millimeter and submillimeter continuum and molecular line observations of the Galactic super star cluster RCW 38, obtained from the Atacama Large Millimeter/Submillimeter Array with a minimum angular resolution of $0''.17 \times 0''.15$ ($\simeq 289\,\mathrm{AU} \times 255\,\mathrm{AU}$). The C$^{18}$O image reveal many massive condensations embedded within filamentary structures extending along the northwest-southeast direction in the center of cluster. The condensations have sizes of 0.01-0.02 pc, $H_2$ column densities of $10^{23}$-$10^{24}$ cm$^{-2}$, and $H_2$ masses of 10-130 $M_\odot$. In addition, the 233-GHz continuum image reveals two dense, small millimeter-sources with radii of 460 and 200 AU (Source A and Source B). Source A is embedded within the most massive C$^{18}$O condensation, whereas no counterpart is seen for Source B. The masses of Source A and Source B are estimated as 13 and 3 $M_\odot$ at the optically-thin limit, respectively. The C$^{18}$O emission shows a velocity gradient of 2 km s$^{-1}$ at the central 2000 AU of Source A, which could be interpreted as a Keplerian rotation with a central mass of a few $M_\odot$ or infall motion of gas. Further, the ALMA $^{12}$CO data reveal that Source A and Source B are associated with molecular outflows exhibiting maximum velocities of ∼30-70 km s$^{-1}$. The outflows have short dynamical timescales of <1000 yr and high mass outflow rates of $\sim 10^{-4}$-$10^{-3}$ $M_\odot$ yr$^{-1}$. These observational signatures suggest an early evolutionary phase of the massive star formation in Source A and Source B.

## 41. SEDIGISM-ATLASGAL: Dense Gas Fraction and Star Formation Efficiency Across the Galactic Disk

**J. S. Urquhart, C. Figura, J. R. Cross, M. R. A. Wells, T. J. T. Moore, D. J. Eden, S. E. Ragan, A. R. Pettitt, A. Duarte-Cabral, D. Colombo, F. Schuller, T. Csengeri, M. Mattern, H. Beuther, K. M. Menten, F. Wyrowski, L. D. Anderson, P. J. Barnes, M. T. Beltrán, S. J. Billington, L. Bronfman, A. Giannetti, J. Kainulainen, J. Kauffmann, M. -Y. Lee, S. Leurini, S. -N. X. Medina, F. M. Montenegro-Montes, M. Riener, A. J. Rigby, A. Sánchez-Monge, P. Schilke, E. Schisano, A. Traficante, M. Wienen** By combining two surveys covering a large fraction of the molecular material in the Galactic disk we investigate the role the spiral arms play in the star formation process. We have matched clumps identified by ATLASGAL with their parental GMCs as identified by SEDIGISM, and use these giant molecular cloud (GMC) masses, the bolometric luminosities, and integrated clump masses obtained in a concurrent paper to estimate the dense gas fractions ($\mathrm{DGF_{gmc}} = \sum M_{\mathrm{clump}}/M_{\mathrm{gmc}}$) and the instantaneous star forming efficiencies (i.e., $\mathrm{SFE_{gmc}} = \sum L_{\mathrm{clump}}/M_{\mathrm{gmc}}$). We find that the molecular material associated with ATLASGAL clumps is concentrated in the spiral arms (∼60searched for variations in the values of these physical parameters with respect to their proximity to the spiral arms, but find no evidence for any enhancement that might be attributable to the spiral arms. The combined results from a number of similar studies based on different surveys indicate that, while spiral-arm location plays a role in cloud formation and HI to $H_2$ conversion, the subsequent star formation processes appear to depend more on local environment effects. This leads us to conclude that the enhanced star formation activity seen towards the spiral arms is the result of source crowding rather than the consequence of a any physical process.

## 42. The asymmetric inner disk of the Herbig Ae star HD 163296 in the eyes of VLTI/MATISSE: evidence for a vortex?

**MATISSE Collaboration, J. Varga et al.** Context. The inner few au region of planet-forming disks is a complex environment. High angular resolution observations have a key role in understanding the disk structure and the dynamical processes at work. Aims. In this study we aim to characterize the mid-infrared brightness distribution of the inner disk of the young intermediate-mass star HD 163296, from VLTI/MATISSE observations. Methods. We use geometric models to fit the data. Our models include a smoothed ring, a flat disk with inner cavity, and a 2D Gaussian. The models can account for disk inclination and for azimuthal asymmetries as well. We also perform numerical hydro-dynamical simulations of the inner edge of the disk. Results. Our modeling reveals a significant brightness asymmetry in the L-band disk emission. The brightness maximum of the asymmetry is located at the NW part of the disk image, nearly at the position angle of the semimajor axis. The surface brightness ratio in the azimuthal variation is $3.5 \pm 0.2$. Comparing our result on the location of the asymmetry with other interferometric measurements, we confirm that the morphology of the $r < 0.3$ au disk region is time-variable. We propose that this asymmetric structure, located in or near the inner rim of the dusty disk, orbits the star. For the physical origin of the asymmetry, we tested a hypothesis where a vortex is created by Rossby wave instability, and we find that a unique large scale vortex may be compatible with our data. The half-light radius of the L-band emitting region is $0.33 \pm 0.01$ au, the inclination is $52^{\circ}{}^{+5^{\circ}}_{-7^{\circ}}$, and the position angle is $143^{\circ} \pm 3^{\circ}$. Our models predict that a non-negligible fraction of the L-band disk emission originates inside the dust sublimation radius for $\mu$m-sized grains. Refractory grains or large ($\gtrsim 10$ $\mu$m-sized) grains could be the origin for this emission.

## 43. On the pumping of the CS($v = 0$) masers in W51 e2e

**D. J. van der Walt, A. Ginsburg, C. Goddi** We present the results of numerically solving the rate equations for the first 31 rotational states of CS in the ground vibrational state to determine the conditions under which the J=1-0, J=2-1 and J=3-2 transitions are inverted to produce maser emission. The essence of our results is that the CS($v = 0$) masers are collisionally pumped and that, depending on the spectral energy distribution, dust emission can suppress the masers. Apart from the J=1-0 and J=2-1 masers the calculations also show that the J=3-2 transition can be inverted to produce maser emission. It is found that beaming is necessary to explain the observed brightness temperatures of the recently discovered CS masers in W51 e2e. The model calculations suggest that a CS abundance of a few times $10^{-5}$ and CS($v = 0$) column densities of the order $10^{16}\,\mathrm{cm}^{-2}$ are required for these masers. The rarity of the CS masers in high mass star forming regions might be the result of a required high CS abundance as well as due to attenuation of the maser emission inside as well as outside of the hot core.

## 44. Constraining the magnetic field properties of Bok globule B335 using SOFIA/HAWC+

**Niko Zielinski, Sebastian Wolf, Robert Brunngräber** Thanks to their well-defined shape and mostly isolated locations, Bok globules are suitable objects for studying the physics of low-mass star formation. To study the magnetic field of the prototypical Bok globule B335, we obtained a spatially resolved polarization map with SOFIA/HAWC+ at a wavelength of $214\,\mu$m. For the first time, these observations reveal that polarization holes in Bok globules, that is, the decrease in polarization degree towards their dense centers, also occur in the far-infrared wavelength regime. The observed polarization pattern is uniform with a mean polarization angle of $48^{\circ} \pm 26^{\circ}$ and a magnetic field strength of $\sim 142\,\mu$G. Moreover, we use complementary polarimetic data for B335 obtained at near-infrared to millimeter wavelengths to analyze and constrain the magnetic field across different scales. By applying the 3D Monte-Carlo radiative transfer code POLARIS (Reissl et al. 2016), we developed a model for the density and magnetic field structure as well as for the dust properties of this globule. We conclude that the column density towards the center of B335 is too low to cause the observed polarization hole in B335 via dichroic absorption (Brauer et al. 2016). Furthermore, we conclude that the effect of self-scattering has no significant impact on the observed polarization. Adopting dust-grain alignment via the radiative torque mechanism, a combination of the interstellar radiation field and the central star as radiation sources is consistent with the decrease in polarization degree at the outer regions of B335 ($\approx 10^4$ au from the core). However, the model fails to explain the low polarization degree within the inner 5000 au.

## 45. Search for associations containing young stars (SACY) VIII. An updated census of spectroscopic binary systems showing hints of non-universal multiplicity among these associations

**S. Zúñiga-Fernández, A. Bayo, P. Elliott, C. Zamora, G. Corvalán, X. Haubois, J. M. Corral-Santana, J. Olofsson, N. Huélamo, M. F. Sterzik, C. A. O. Torres, G. R. Quast, C. H. F. Melo** We seek to update the spectroscopy binary fraction of the SACY (Search for Associations Containing Young stars) sample taking in consideration all possible biases in our identification of binary candidates, such as activity and rotation. Using high-resolution spectroscopic observations we have produced ∼1300 cross-correlation functions (CCFs) to disentangle the previously mentioned sources of contamination. The radial velocity values obtained were cross-matched with the literature and were used to revise and update the spectroscopic binary (SB) fraction in each of the SACY association. In order to better describe the CCF profile, we calculated a set of high-order cross-correlation features to determine the origin of the variations in radial velocities. We identified 68 SB candidates from our sample of 410 objects. Our results hint that the youngest associations have a higher SB fraction. Specifically, we found sensitivity-corrected SB fractions of $22^{+15}_{-11}\%$ for $\epsilon$ Cha , $31^{+16}_{-14}\%$ for TW Hya and $32^{+9}_{-8}\%$ for $\beta$ Pictoris, in contrast with the five oldest ($\sim 35 - 125$ Myr) associations we have sampled which are $\sim 10\%$ or lower. This result seems independent of the methodology used to asses membership to the associations. The new CCF analysis, radial velocity estimates and SB candidates are particularly relevant for membership revision of targets in young stellar associations. These targets would be ideal candidates for follow-up campaigns using high-resolution techniques in order to confirm binarity, resolve the orbits, and ideally calculate dynamical masses. Additionally, if the results on SB fraction in the youngest associations are confirmed, it could hint of non-universal multiplicity among SACY associations.